CORE
Metadata, citation and similar papers at core.ac.uk
Provided by CERN Document Server

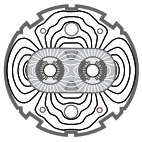

LHC Project Note 413

2008-03-04

Alexej.Grudiev@cern.ch

Simulation and reduction of longitudinal and transverse impedances of a collimation device with two beams in one vacuum chamber

A. Grudiev / AB-RF

Keywords: Broad-band impedance, longitudinal impedance, transverse impedance, trapped modes, collimator, TCLIA, TCTVB

Summary

The results of simulation of trapped modes in a collimation device with two beams in one vacuum chamber for LHC are presented. Both monopole and dipole modes have been analyzed giving estimates of the longitudinal and transverse impedances for different values of the collimator gap. In addition the low frequency broad-band longitudinal and transverse impedances have analyzed and several measures for its reduction have been proposed.

1. Introduction

Due to lack of space, some of vertical tertiary collimators (TCTVBs) and injection protection devices (TCLIAs) must be positioned at about 75 m from the IPs in IR2 and IR8. The vacuum chamber at these locations has larger horizontal aperture (~180 mm) to accommodate both proton beams, as well as the ALICE ZDC spectator protons. The TCS (secondary collimator) design [1] cannot be used because it provides aperture only for single proton beam; a new design is necessary. Altogether, there are 6 collimation devices of this type: 4 TCTVBs, 2 on either side of the IPs in IR2 and IR8, and 2 TCLIAs at both injection locations at IR2 and IR8. Final locations of the devices and some of the requirements on the aperture can be found in Ref. [2]. All 6 devices have the same design. The only difference is that the TCTVB has W jaws whereas TCLIA has C jaws.

In order to minimize the cost of the new collimation device, the design of the TCS type has been adopted as much as possible. This resulted in the first version of the design proposed by the Collimation Working Group (CWG) [3], which will be referred to as “initial design” in the following. This design is a combination of the collimation jaws of the TCS design with a new beam screen of the size of the larger vacuum chamber to provide both the required aperture and the smooth path for the beam image currents.

In this note, we present the results of the numerical simulations of transverse and longitudinal impedances of the initial design. The impact of the calculated impedances on the device performance and on the beam stability is discussed. Furthermore, several changes to the design are proposed in order to reduce the impedances of the device. Finally, the impedances of the improved design are calculated.

This is an internal CERN publication and does not necessarily reflect the views of the LHC project management.

2. Longitudinal and transverse impedances of the initial design

This section is organized as follows: First, the geometry of the initial design proposed by the CWG is described in subsection 2.1, as well as its implementation in the numerical simulation codes used for impedance simulations. Then, the longitudinal and transverse impedances of the initial design are calculated and discussed in subsections 2.2 and 2.3, respectively. Finally, the results are summarized and the necessity to change the initial design is addressed in subsection 2.4.

2.1 Geometry of the initial design

The initial design consists of a pair of collimation jaws of the TSC design in a stainless steel vacuum tank of nearly square cross-section. The length of the device is about the same as the length of the TSC. The upper half of the cross-section is shown in Fig. 1. The vacuum tank is large enough to provide the required horizontal aperture of ~180 mm. The required vertical aperture is about 70 mm resulting in elliptical cross-section beam pipes at both extremities of the device. In order to provide a smooth path for the beam image currents, a copper beam screen of the same elliptical cross-section connects the beam pipes. The beam screen has two slots to introduce the jaws inside of the aperture region. There are two sets of silver-plated rf-fingers per jaw to provide electrical contact between the jaw and the beam screen, which is necessary to keep beam excited wake-fields inside the beam screen. These transverse rf-fingers are shown in Fig. 1. There are two other sets of silver-plated rf-fingers per jaw, which connect the jaw with the beam pipes at both ends of the jaw. Together with the 15-degree tapers at each end of the jaw, they provide a smooth path for the beam image currents in the region of the jaw. Fig. 2 is a three-dimensional view of ¼ of the device, showing these longitudinal rf-fingers.

The jaws can be retracted to provide the full aperture of 60 mm or they can be closed to collimate the beam. The smallest gap which is required in the case of TCTVB is 2.6 mm [4]. Since the two jaws can be moved independently, the device is not always symmetric with respect to the horizontal plane. However, we did not consider this case. In this note, the impedances are calculated for a symmetric device with the gap between the jaws in the range from 60 mm to 3 mm.

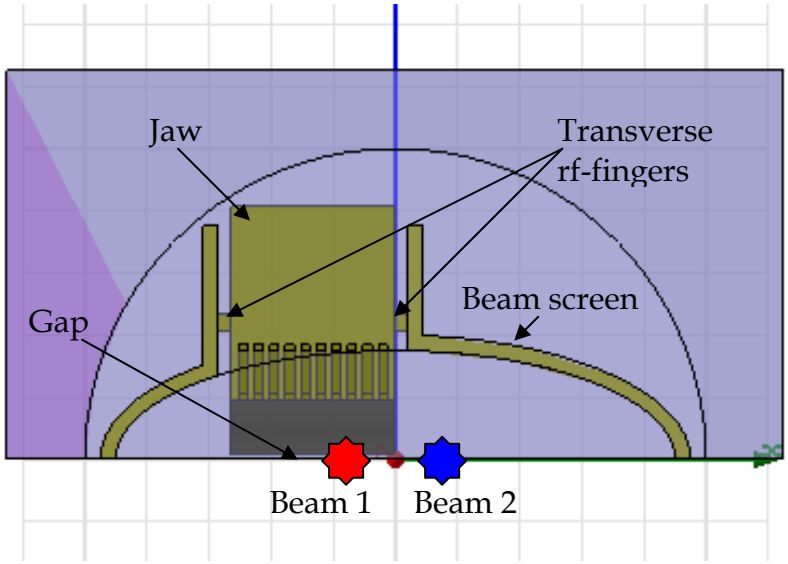

Figure 1 Cross-section of the initial design showing the transverse rf-fingers.

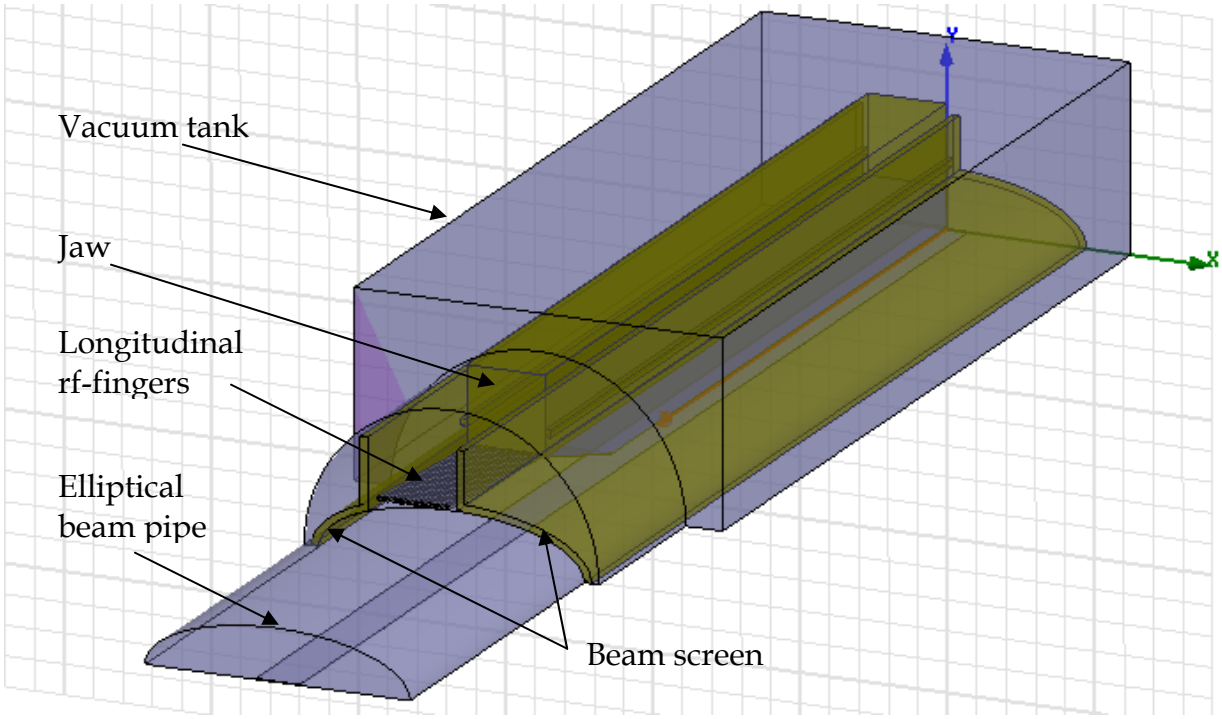

Figure 2 Three-dimensional view of ¼ of the initial design showing the longitudinal rf-fingers.

A 3-D model of the initial design has been implemented in HFSS [5] I, a numerical code for frequency-domain simulation of electromagnetic fields. The results of the implementation are shown in Fig. 2. Only the details relevant for rf properties of the device are described. Moreover, only a part of the full geometry with appropriate boundary conditions applied at the symmetry planes is usually simulated: ¼ in HFSS and ½ in GdfidL. Simulations have been done usually as following: The 3D model has been exported from HFSS to GdfidL [6], a time-domain code for wake-field simulations. Geometrical impedance versus frequency curve has been calculated using GdfidL in a very wide frequency range from DC to the cut-off frequency of the bunch spectrum. This impedance curve gives both the broad-band geometrical impedance of the device at low frequencies and the frequencies of the trapped modes. Knowing their frequencies, the trapped modes are subsequently simulated using HFSS and their relevant parameters calculated.

2.2 Longitudinal impedance of the initial design

Applying magnetic wall boundary condition at the horizontal symmetry plane, the longitudinal (monopole) geometrical impedance was calculated in GdfidL for the full range of the collimation gap from 3 mm to 60 mm. Fig. 3 shows the real and imaginary parts of the impedance seen by beam 1, which means that the corresponding wake is excited and integrated at the transverse position of beam 1 (see Fig. 1). In Fig. 4, the same quantities are presented for beam 2. The low frequency part of the imaginary part of the impedance curve, which has nearly linear frequency dependence, was used to calculate Z/n for different values of the gap. The dependence of this parameter on the gap size is shown in Fig 5 for both beams. The smaller the gap, the higher is the longitudinal broad-band geometrical impedance of the device. The dependence on the gap is much stronger for beam 1, which is explained by its position directly between the jaws.

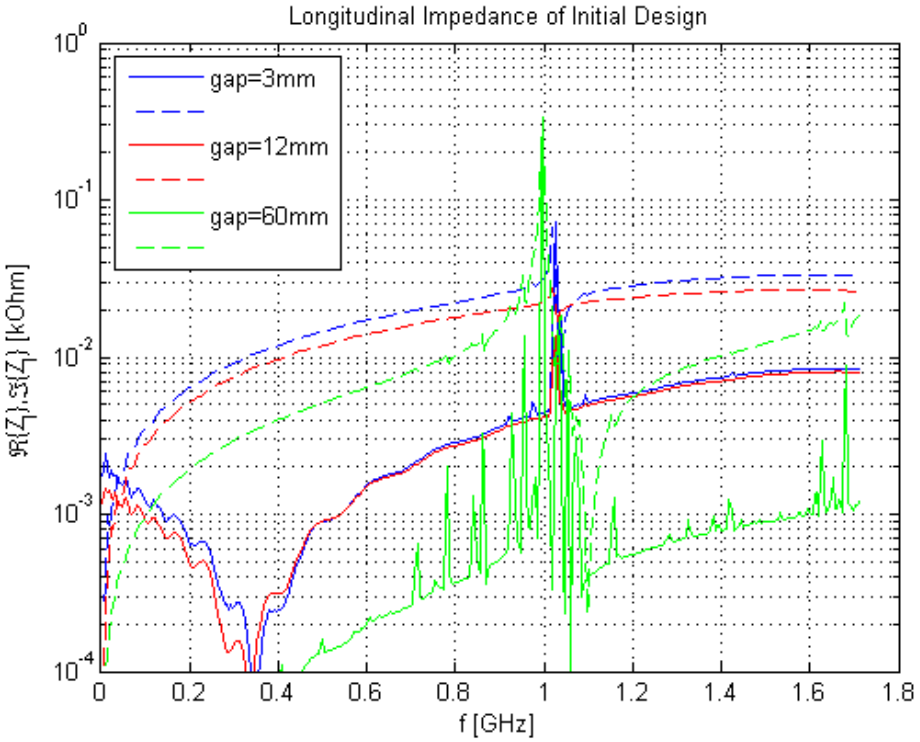

Figure 3 Real (solid lines) and imaginary (dashed lines) parts of the longitudinal impedance of the initial design for 3 different values of the collimation gap: 3 mm, 12 mm and 60 mm. The wake is excited and integrated at the position of beam 1 (see Fig. 1).

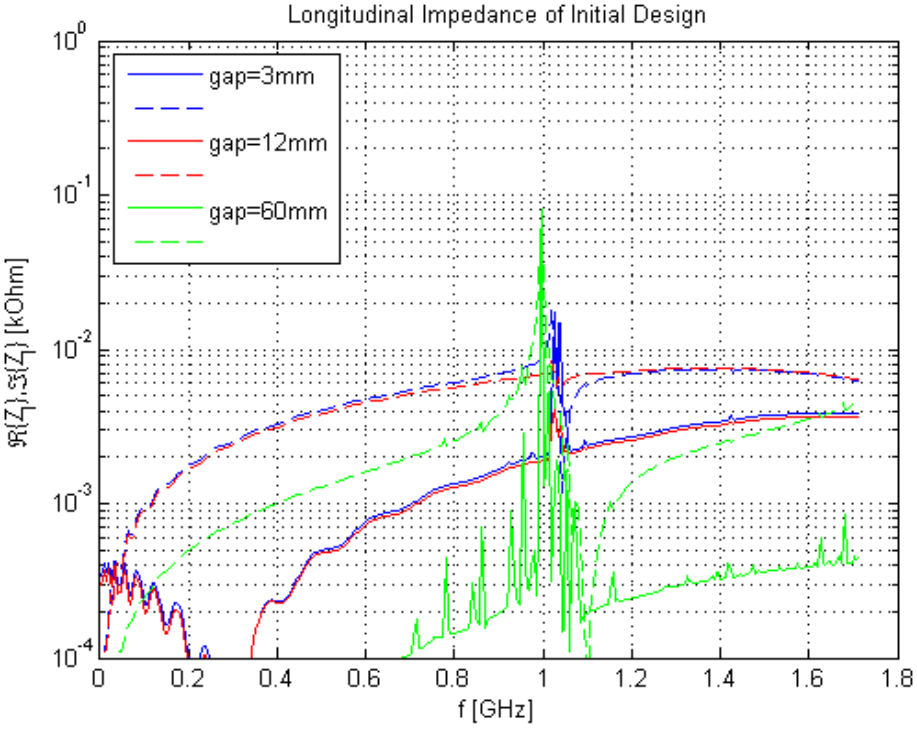

Figure 4 Real (solid lines) and imaginary (dashed lines) parts of the longitudinal impedance of the initial design for 3 different values of the collimation gap: 3 mm, 12 mm and 60 mm. The wake is excited and integrated at the position of beam 2 (see Fig. 1).

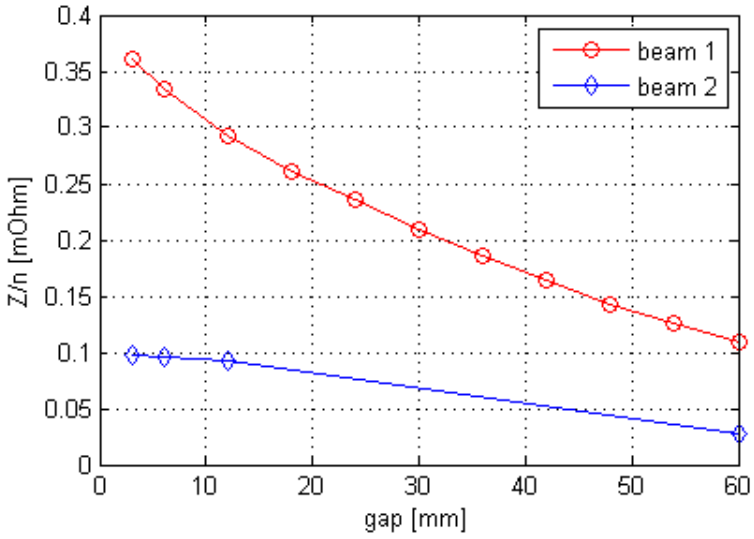

Figure 5 Longitudinal broad-band geometrical impedance of the initial design versus gap for both positions of the beam: 1 (red) and 2 (blue).

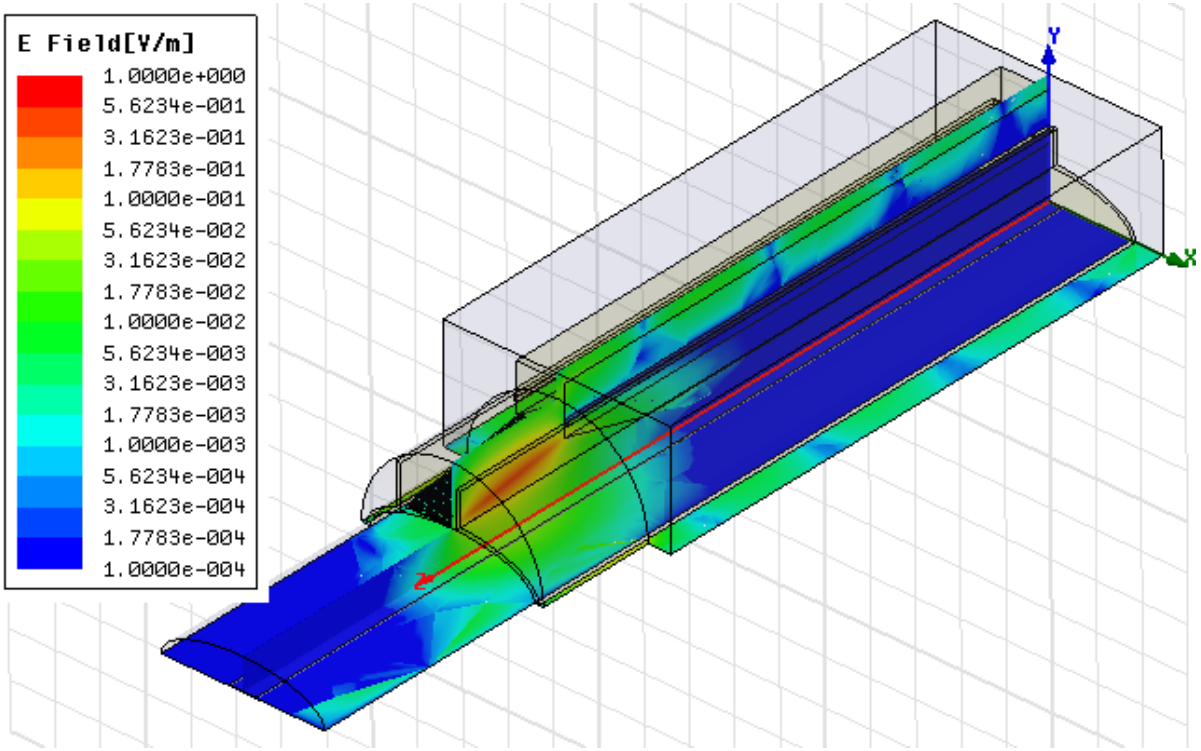

Figure 6 Distribution of electric field for the most dangerous monopole trapped mode.

From the real part of the impedance, frequencies of the trapped modes were determined. They are located mainly around 1 GHz. Since no losses are included in the time-domain simulations, the shunt impedance cannot be calculated directly from the height of the peaks in the real part of the impedance curve. On the other hand, the height of the peaks is proportional to the loss factor of corresponding modes. Keeping this in mind, a few remarks can be made: First, the trapped mode with the highest loss factor has frequency very close to 1 GHz for the gap of 60 mm. Second, in contrast to the broad-band impedance, as the gap is reduced, the loss factor of the trapped modes decreases.

That is why, in order to get an upper estimate on the power loss due to a single trapped mode, the most dangerous mode with the highest loss factor has been identified at about 1 GHz for gap of 60 mm. Both beam 1 and beam 2 excite the same trapped mode, but the loss factor of the mode calculated at the position of beam 1 is larger than if calculated at the position of the beam 2. Knowing the frequency of the most dangerous mode, the other parameters of this mode have been calculated using HFSS: frequency f_0=0.996 GHz, quality factor Q_0=2550 (for TCTVB with W jaws), shunt impedance R_0^{b1}=3.5 kΩ at the position of beam 1 and R_0^{b2}=0.87 kΩ at the position of beam 2. In Fig. 6, the distribution of the electric field of this mode is shown, demonstrating that the field is trapped in the transition region from beam pipe to the jaws. Modes trapped in this region are the most dangerous because they cause heating of the longitudinal rf-fingers, which are probably the most delicate part of the device. It is important to calculate how much of the total power loss is absorbed by each rf-finger. In Fig. 7, the surface density of power loss on the rf-fingers is shown; it is different for each rf-finger. For the most dangerous mode, the largest amount of the power loss is dissipated on the surface of the vacuum tank. Nevertheless, about 0.65 % is dissipated on the hottest rf-finger (the rightmost in Fig. 7).

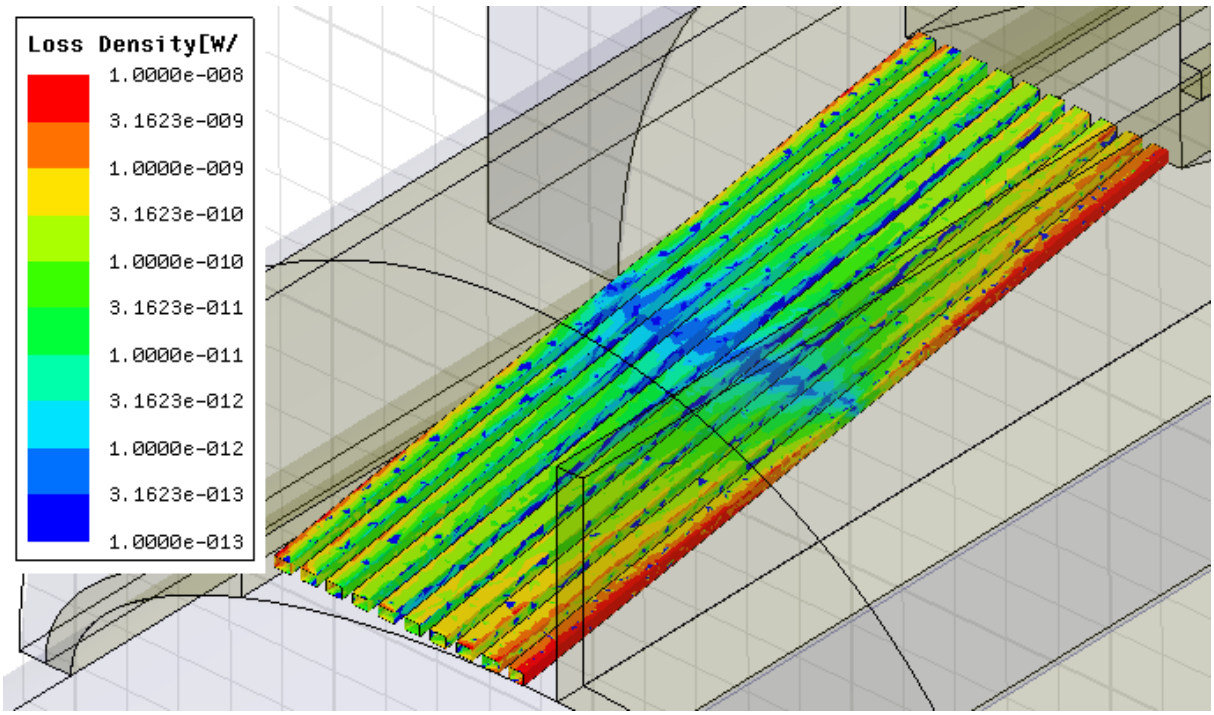

Figure 7 Power loss density on the surface of one set of longitudinal rf-fingers for the most dangerous monopole trapped mode.

2.3 Transverse impedance of the initial design

Applying electric wall boundary condition at the horizontal symmetry plane, transverse (dipole) geometrical impedance was calculated in GdfidL for the full range of the collimation gap from 3 mm to 60 mm. Fig. 8 shows the real and imaginary parts of the transverse impedance calculated at the position of beam 1 for gap of 3 mm, 12 mm and 60 mm and at the position of beam 2 for gap of 3 mm. The imaginary part of the impedance approaches a constant value as frequency goes to 0. This limiting value: $\Im\{Z_y\}\big|_{f=0}$ is plotted in Fig 9 for different gap sizes at the position of the beam 1. The smaller the gap, the higher is the transverse broad-band geometrical impedance of the device.

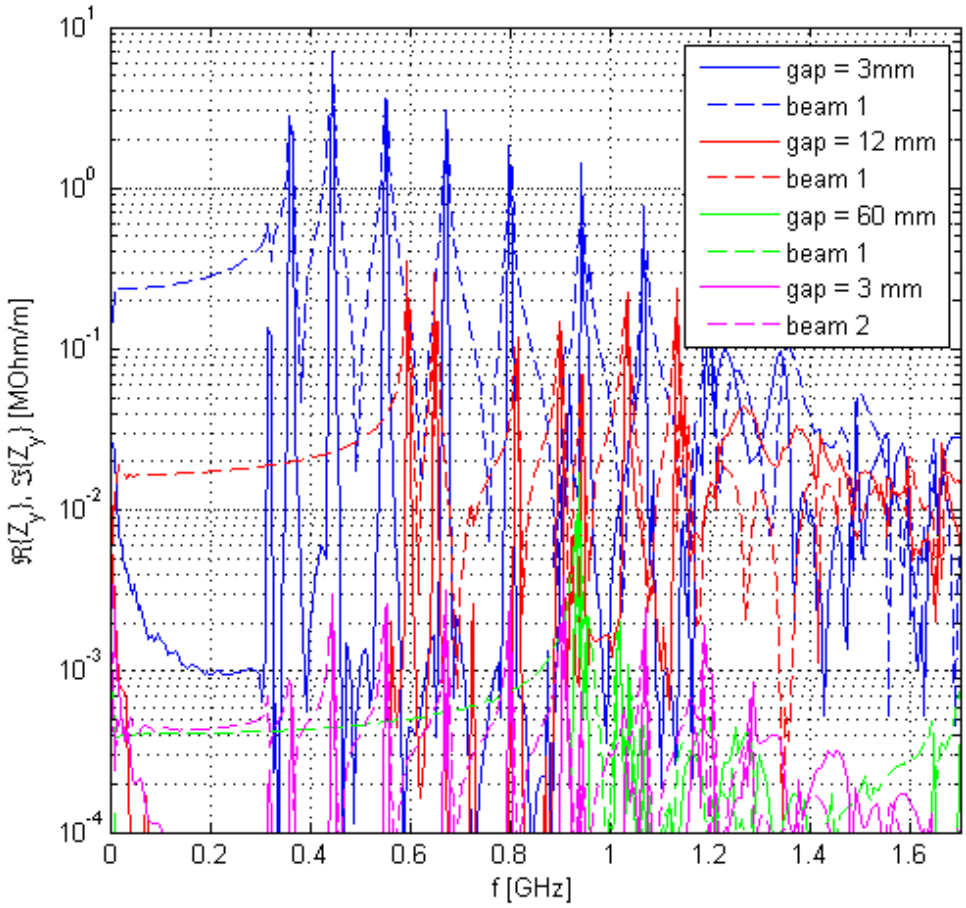

Figure 8 Real (solid lines) and imaginary (dashed lines) parts of the transverse impedance of the initial design for 3 different values of the collimation gap: 3 mm, 12 mm and 60 mm are shown in blue, red and green, respectively. For this set of curves, the wake is excited and integrated at the position of beam 1 (see Fig. 1). Magenta lines represent the real and imaginary parts of the transverse impedance for the gap of 3 mm at the position of beam 2.

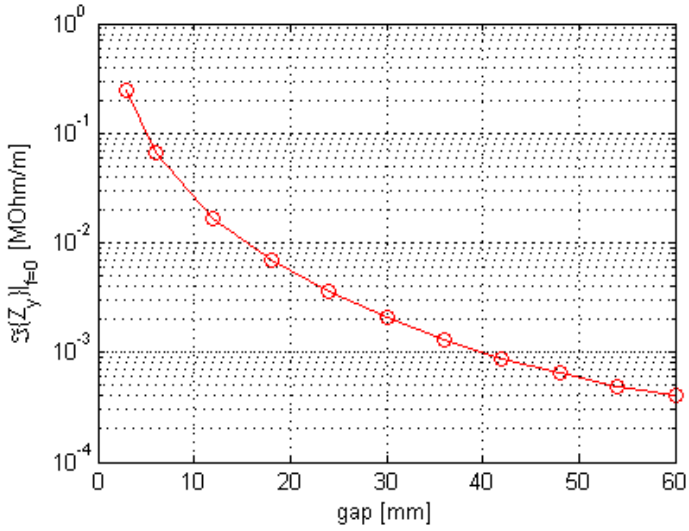

Figure 9 Transverse broad-band geometrical impedance of the initial design versus gap for positions of the beam 1.

Table 1. Parameters of the first 6 modes in TCTVB for gap of 3 mm at the position of beam 1.

Mode #	Frequency [GHz]	Quality factor	Transverse impedance [MΩ/m]
1	0.317	3080	16.6
2	0.362	1700	153
3	0.443	1080	174
4	0.551	920	81
5	0.671	880	42
6	0.799	810	18

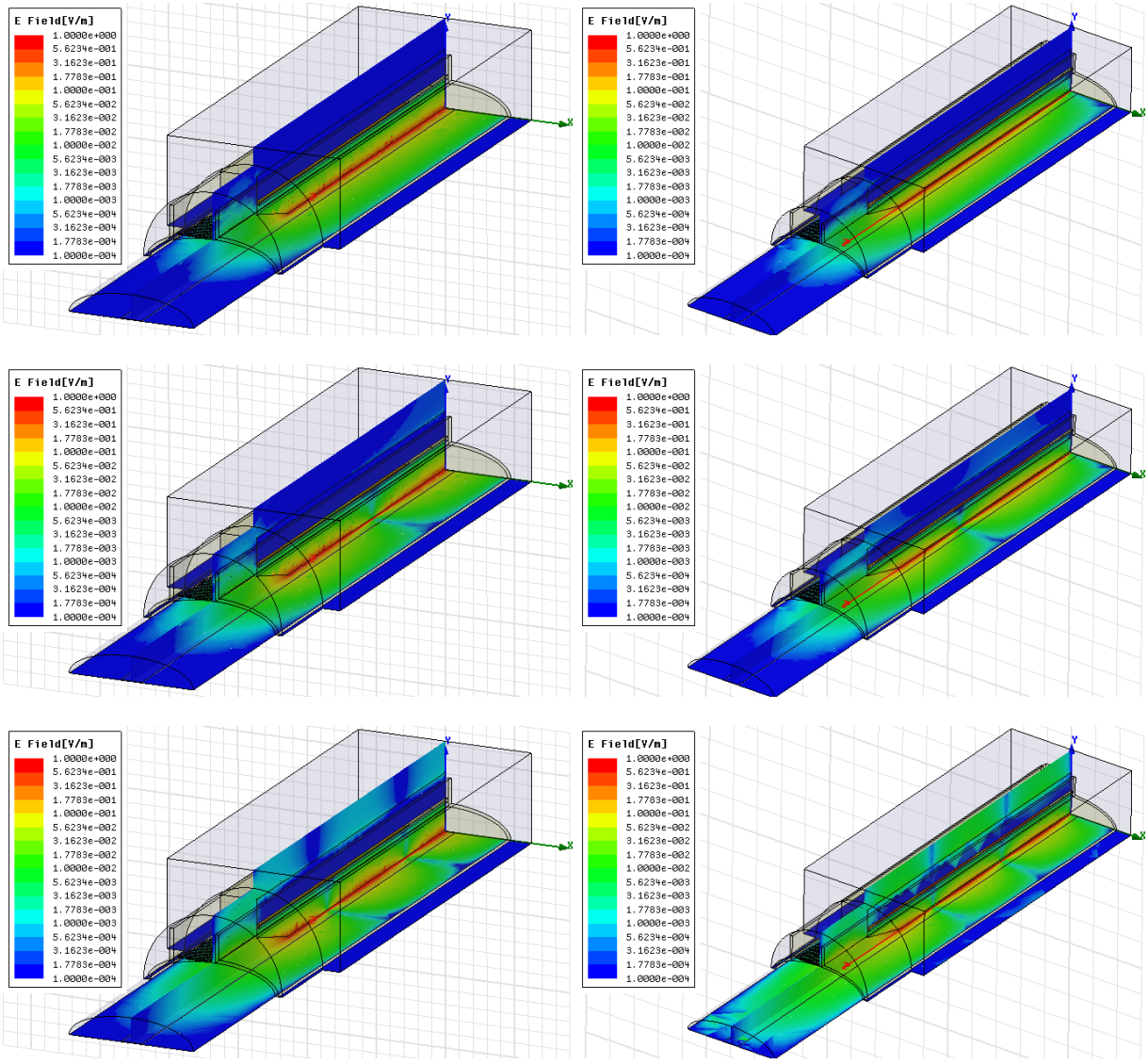

Figure 10 Electric field distributions of the first 6 modes in TCTVB for gap of 3 mm at the position of beam 1.

From the real part of the impedance curves presented in Fig 8, frequencies of the dipole trapped modes were determined. The height of the peaks is proportional to the kick factor of the modes. As for the broad-band impedance, the modes for 3 mm gap have the highest kick factors. They are coupled much stronger to beam 1 than to beam 2 (compare blue and magenta lines in Fig. 8). Moreover, the larger the gap, the higher are the trapped mode frequencies, which further reduces coupling to the beam. For these two reasons, in order to calculate the worst case, the first six trapped modes with frequencies in the range from 0.3 GHz to 0.8 GHz have been simulated in HFSS for a gap of 3 mm at the position of beam 1. In Fig. 10 the electric field distribution of these modes is shown. All modes have a similar structure of the electromagnetic field, which is that of the ridged waveguide: the electric field is concentrated in the gap between the jaws (ridges), where beam 1 passes the device. This is why beam 1 is strongly coupled to these modes. The magnetic field is distributed in the whole space on both sides of the jaws, such that associated currents flow mostly on the copper beam screen. This is the reason why these modes have a rather high quality factor of about 1000. The difference between the modes is the number of variations of the electromagnetic field along the jaws. This number of longitudinal variations corresponds to the mode number in Table 1, where the parameters of the modes are summarized.

2.4 Impact of the impedance of the initial design on device performance and beam stability

In this subsection, the impact of the impedance of the initial design calculated above is estimated and conclusions about acceptability of the device are drawn. In Table 2 some parameters of the LHC beam at nominal intensity are presented, which were used in this note.

Table 2. Some parameters of the LHC beam at nominal intensity used in this note.

Bunch charge: q [nC]	16
Bunch repetition frequency: f_b [MHz]	40
Bunch length (Gaussian RMS): σ_z [mm]	80
LHC revolution frequency f_{rev} [kHz]	11.245
Average beta-function $\langle\beta\rangle$ [m]	70

2.4.1 Heating due to the monopole trapped mode

Assuming the worst case, when the frequency of the most dangerous trapped mode coincides with one of the harmonics of bunch repetition frequency,

$$f_0 = nf_b, \tag{1}$$

the power loss of a single beam is estimated as

$$P_0 = I_0^2 \cdot 2R_0, \tag{2}$$

where R_0 is R_0^{b1} or R_0^{b2} depending on the position of the beam, $I_0 = q f_b \exp(-(\omega_0 \sigma_z / c)^2 / 2)$, $\omega_0 = 2\pi f_0$ and c is the speed of light. From (1), the power loss at the position of beam 1 and 2 are 174 W and 43 W, respectively.

If two beams are circulating at the same time the situation is more complicated. Depending on the relative phase between the bunches of beam 1 and beam 2, the power loss can be lower or higher than the single beam power loss. To consider this situation, let us introduce 4 new variables. Two complex currents: $I_0^{b1} = I_0 \exp(i\varphi^{b1})$ and $I_0^{b2} = -I_0 \exp(i\varphi^{b2})$ for beam 1 and beam 2, respectively (here φ^{b1} and φ^{b1} are phases of beam 1 and 2, respectively) and two complex voltages: $V_0^{b1} = \int_{b1} E_z \exp(i\omega_0 z/c) dz$ and $V_0^{b2} = \int_{b2} E_z \exp(i\omega_0 z/c) dz$, which are two integrals of the longitudinal electric field seen by beam 1 and 2, respectively. Then by definition we have:

$$\begin{pmatrix} V_0^{b1} \\ V_0^{b2} \end{pmatrix} = \begin{bmatrix} Z_{11} & Z_{12} \\ Z_{21} & Z_{22} \end{bmatrix} \begin{pmatrix} I_0^{b1} \\ I_0^{b2} \end{pmatrix}, \tag{3}$$

and the power loss in the presence of both beams can be calculated as

$$P_0 = \begin{pmatrix} V_0^{b1} & V_0^{b2} \end{pmatrix} \cdot \begin{pmatrix} I_0^{b1} \\ I_0^{b2} \end{pmatrix}^*, \tag{4}$$

In the worst case, when (1) holds, the impedance-matrix in (3) is real and the terms can be expressed using peak impedances of the mode calculated at the position of beam 1 and 2 as:

$$Z_{11} = 2R_0^{b1}; \quad Z_{22} = 2R_0^{b2}; \quad Z_{12} = Z_{21} = 2\sqrt{R_0^{b1} R_0^{b2}}, \tag{5}$$

Then substituting (3) and (5) into (4), the power loss is expressed as

$$P_0 = I_0^2 \cdot 2\left(R_0^{b1} + R_0^{b2} - 2\sqrt{R_0^{b1} R_0^{b2}} \cos(\delta\varphi)\right), \tag{6}$$

where $\delta\varphi = \varphi^{b1} - \varphi^{b2}$ is the phase difference between the two beams. Assuming that it is 0 at the IP, it can be calculated at any distance δs from the IP as $\delta\varphi = \omega_0 2\delta s / c$. For the most dangerous mode with frequency of 1 GHz, the cosine changes its sign every 75 mm of longitudinal displacement of the device. In this case, the power loss varies between 391 W ($\cos(\delta\varphi) = -1$) and 44 W ($\cos(\delta\varphi) = 1$). Correspondingly, the power loss in the hottest rf-finger varies between 2.5 W and 0.3 W. To be on the safe side and do not depend on the device position and beam structure, the largest value must be considered. 2.5 W per rf-finger is very high and would lead in vacuum and for rf-fingers of the type used in TCS collimators [7] to a temperature increase of at least several hundred K. For this reason, the shunt impedance of the trapped mode must be reduced.

2.4.2 Broad-band geometrical impedance

According to [2] and [4] there will be 4 TCTVB with minimum gap of about 3 mm at top energy and 60 mm at injection, and 2 TCLIA with gap of about 12 mm at injection and 60 mm

at top energy. Moreover, each beam passes through one TCLIA and two TCTVBs at the position of beam 1, and through another TCLIA and two others TCTVBs at the position of beam 2.

Taking the value from Fig. 5 for corresponding gaps and beam positions, the contributions of all 6 devices to longitudinal broad-band impedance of LHC is estimated to be 0.66 mΩ at injection and 1.06 mΩ at top energy. This is an acceptable but not negligible increase of the total LHC impedance budget estimated in [8] to be 70 mΩ at injection and 76 mΩ at top energy.

Since the transverse broad-band impedance of the device at minimum gap size and at position of beam 1 dominates all other contributions (60 mm gap and/or position of beam 2), only one TCLIA with gap of 12 mm at injection and two TCTVB with gap of 3 mm at top energy are taken into account to estimate the contribution to the transverse broad-band impedance of the LHC. Hence taking the value from Fig. 9 and multiplying it with the ratio of local beta-function (~55 m for TCTVBs and ~127 m for TCLIAs) [4] to $\langle\beta\rangle$, the contribution is estimated to be 0.04 MΩ/m at injection and 0.47 MΩ/m at top energy. The total LHC broad-band impedance estimated in [8] is 1.34 MΩ/m at injection and 2.67 MΩ/m at top energy. Certainly, an increase of the budget by nearly 20 % at top energy is a substantial change and must be justified. In any case, a reduction of the transverse broad-band geometrical impedance of the device is absolutely necessary, in order not to increase the budget significantly.

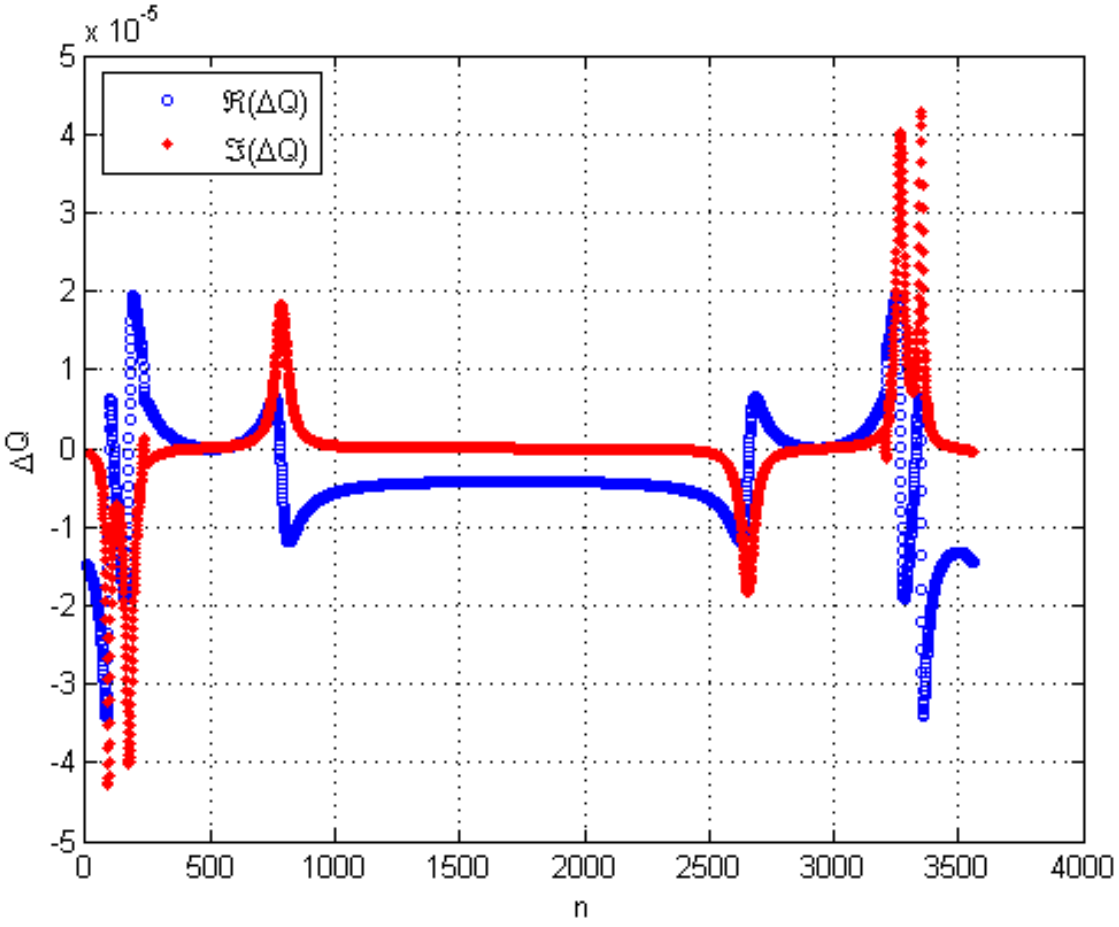

Figure 11 Real (blue) and imaginary (red) parts of transverse coupled bunch instability tune shift due to dipole trapped modes with parameters presented in Table 1.

2.4.3 Transverse coupled-bunch instability due to dipole trapped modes

To estimate the transverse coupled-bunch instability tune shift due to dipole trapped modes, the parameters of which are presented in Table 1, formula (4.114) from [9] is used. This formula was modified to take into account finite bunch lengths (factor $\exp(-(\omega'\sigma_z/c)^2)$ and local beta-functions (factor 55/70, see subsection 2.4.2). In addition to the parameters mentioned in Table 2, a vertical tune of 59.31 and zero chromaticity were assumed. The results are presented in Fig. 11. There are two beam modes with very close mode numbers 3267 and 3350. These modes have also very close values of the imaginary part of the tune shift: 0.4×10^{-4} and 0.42×10^{-4}, respectively. Beam mode number 3267 couples to the dipole mode number 3 from Table 1, whereas beam mode number 3350 to the dipole mode 2. Fig. 8 confirms that changing the gap size changes frequencies of the dipole modes. Thus we can assume that a frequency difference between dipole mode 2 and 3 may become a harmonic of the bunch repetition frequency, in which case both modes 2 and 3 will couple to the same beam mode. The imaginary part of the tune shift in this case will be the sum of the two: 0.82×10^{-4}, which is not much below the stability limit of 1.5×10^{-4} for maximum Landau octupole current at top energy [10]. Hence it very desirable to reduce the impedance of the dipole trapped modes to an acceptable level below 1 MΩ/m.

2.4.4 Summary of the findings concerning the initial design

- An increase of the longitudinal broad-band impedance by 0.66 mΩ at injection and 1.06 mΩ at top energy is acceptable.

- An increase of the transverse broad-band impedance by 0.04 MΩ/m at injection and 0.47 MΩ/m at top energy is not acceptable. A reduction to a level of about 1 % of the total LHC budget (0.014 MΩ/m and 0.028 MΩ/m, respectively) is strongly recommended.

- Both overall power loss of 391 W in the whole device and the local heating of rf-fingers of 2.5 W due to monopole trapped modes are too high and must be reduced by at least factor 10.

- The coupled-bunch instability tune shift only due to dipole trapped modes is very close to the stability limit. Taking into account all other sources of impedance in the LHC can lead to the loss of stability. It is strongly recommended to reduce the impedance of the dipole modes by at least factor 10.

In summary, almost all types of the initial design impedance must be reduced. A number of substantial changes to the initial design have to be done.

3 Improved design

In this section, different proposals for design improvement in order to reduce the device impedance are analyzed. Finally, the impedance of the improved design is calculated.

3.1 Device improvement

3.1.1 Reduction of the transverse broad-band impedance

There are different ways to achieve transverse broad-band impedance reduction. According to [11, 12], the transverse impedance of a flat collimator with a small tapering angle α has the following dependence on the geometrical parameters:

$$Z_y \sim \alpha h(1/a - 1/b) \tag{7}$$

where h, a and b are the width, gap and beam pipe size of the collimator, respectively. Though the geometry of our device is more complicated than that of a simple flat collimator, we can expect the same dependence of the transverse impedance on the geometrical parameters. Moreover, reduction of the transverse broad-band impedance helps also to reduce R/Q of the trapped modes.

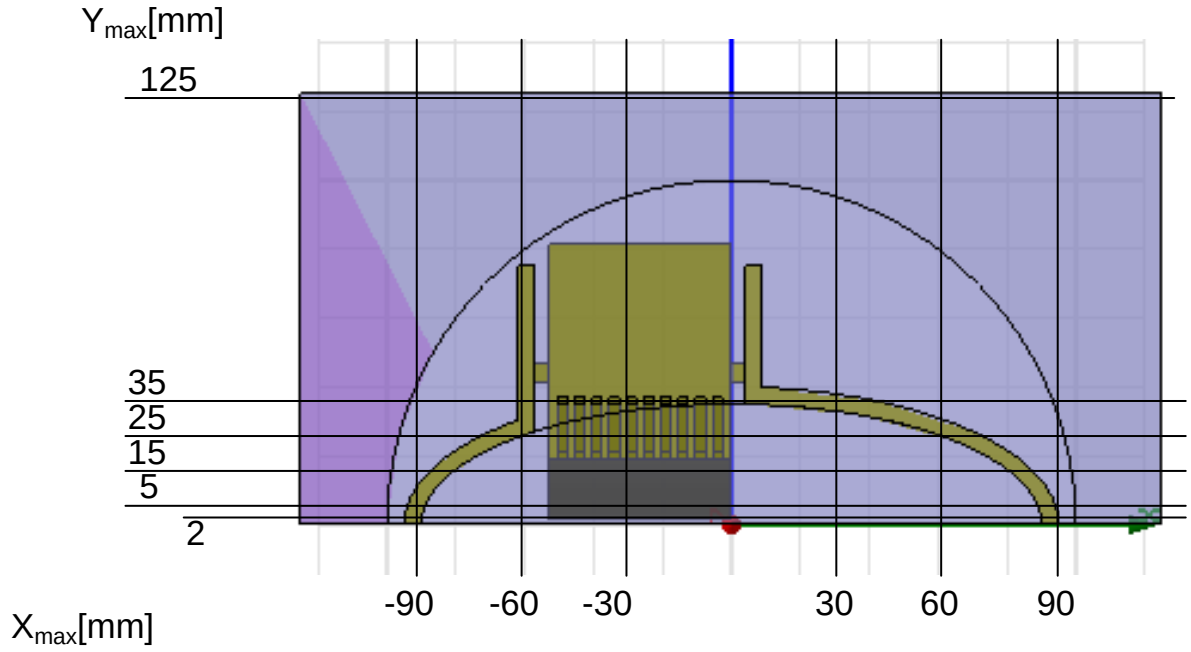

Figure 12 Cross-section of the device with vertical and horizontal cutting planes used to reduce the size of the device aperture. The size of the gap is 3 mm.

First, the dependence of the transverse impedance on the size of the aperture was studied. The size of the cross-section of the device was reduced step by step as shown in Fig. 12 by cutting off external part of the device. In each case, transverse geometrical impedance of the device was calculated using GdfidL. In Table 3, the transverse broad-band impedance is presented for each case. The first 6 rows show the dependence of the impedance on the vertical size of the vacuum tank and the beam screen aperture. No significant reduction of the impedance is demonstrated unless the aperture is very small (below 15 mm), which is not acceptable. The last 3 rows show the dependence of the impedance on the horizontal aperture of the beam screen. The transverse broad-band impedance of the device is roughly proportional to the horizontal aperture and can thus be significantly reduced by decreasing the horizontal aperture. Unfortunately, horizontal aperture cannot be reduced because it must accommodate two beams together with the ALICE ZDC spectator protons as discussed in the Introduction. In fact, the much higher impedance of the initial design of the device compared to the TCS collimator design, which has been calculated in [13], is mainly the result of this bigger horizontal aperture.

Table 3. Transverse broad-band (BB) geometrical impedance for different positions of cutting planes which are shown in Fig. 12. The size of the gap is 3 mm.

X_{max}[mm]	Y_{max}[mm]	Transverse BB impedance [MΩ/m]
[-90, 90]	125	0.232
[-90, 90]	35	0.23
[-90, 90]	25	0.22
[-90, 90]	15	0.177
[-90, 90]	5	0.081
[-90, 90]	2	0.012
[-60, 60]	25	0.15
[-30, 30]	25	0.063
[-30, 0]	25	0.046

Another way of reducing the transverse broad-band impedance is to modify the shape of the tapers, which can be done in two ways: decreasing the tapering angle α, which is 15 degree in the initial design, and/or making the taper non-linear, which according to [11] can reduce the impedance by as much as factor 2 in certain cases. Fig 13 shows geometry of the tapering region of the initial design for 15-degree linear taper and 10-degree linear and non-linear tapers. In addition, 7-degree linear and non-linear tapers were calculated. The results are summarized in Table 4. The reduction of the tapering angle decreases the transverse impedance slightly, it is however not enough to reach the goal specified in Subsection 2.4.4. Nevertheless, a 10-degree linear taper is recommended for an improved design also because of the smoother tapering compared to the 15-degree linear taper (see Fig. 13 (a) and (b)). Non-linear tapers do not give enough reduction of the transverse impedance to justify their increased complexity.

Table 4. Transverse broad-band (BB) geometrical impedance for different geometries of the taper. The size of the gap is 3 mm.

Taper type	Taper angle [^{o}]	Transverse BB impedance [MΩ/m]
Linear	15	0.235
Linear	10	0.214
Linear	7	0.196
non-linear	10	0.200
non-linear	7	0.192

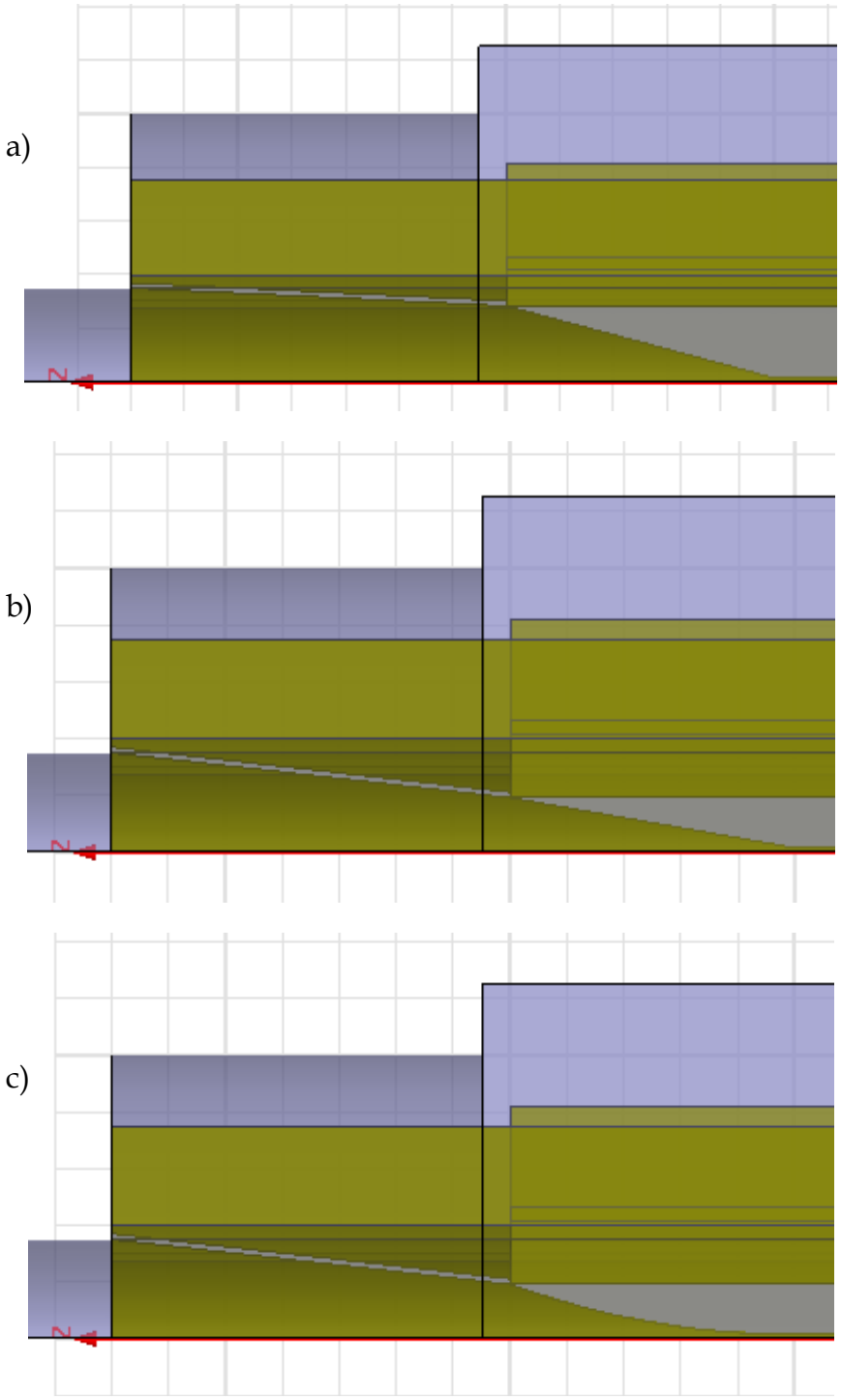

Figure 13 Geometry of taper region of the initial design for 15-degree linear and 10-degree linear and non-linear tapers are shown in (a), (b) and (c), respectively. The size of the gap is 3 mm.

Since the large aperture cannot be reduced and the reduction of the impedance due to taper improvement is small compared to what is necessary, the only option left is to increase the gap size. Both Eq. (7) and Fig. 9 demonstrate a strong dependence of the transverse broad-band impedance on the gap size. In order to satisfy the requirement summarized in subsection 2.4.4 and not exceed 1 % of total LHC impedance budget the minimum allowed gap of the

device at top energy must be increased up to 12 mm. This decreases the transverse impedance by more than a factor 10 and results in the transverse broad-band impedance of two TCTVBs at top energy of about 0.024 MΩ/m, which is slightly below 1 % of the total LHC broad-band impedance budget. This also reduces the longitudinal broad-band impedance of all 6 devices at top energy from 1.06 mΩ to 0.9 mΩ.

3.1.2 Reduction of the transverse impedance of the dipole trapped modes

All measures for reduction of the transverse broad-band impedance, which are described in the previous subsection also reduce R/Q of the dipole trapped modes and hence the impedance of the dipole modes. But this is not enough. Another way to reduce the impedance of these modes is to damp them by introducing losses. In Fig 10, the structure of electric field of the dipole modes is shown. The electromagnetic field of the modes is confined inside the beam screen. Since the main purpose of the beam screen is to reduce the ohmic losses for the beam image currents, we cannot simply put lossy material inside; it would increase the resistive wall impedance of the device. A special place for lossy material is necessary, hidden from the beam but not from the dipole trapped mode fields. A solution is the introduction of a special damping chamber filled with ferrite blocks, parallel to the beam screen. The chamber shields the ferrite from the beam image currents. On the other hand, the dipole trapped modes are very well coupled to the chamber and damped by the ferrite. The cross-section of the modified beam screen and the ferrite is shown in Fig. 14. This damping chamber goes along the whole device as is shown in Fig. 15.

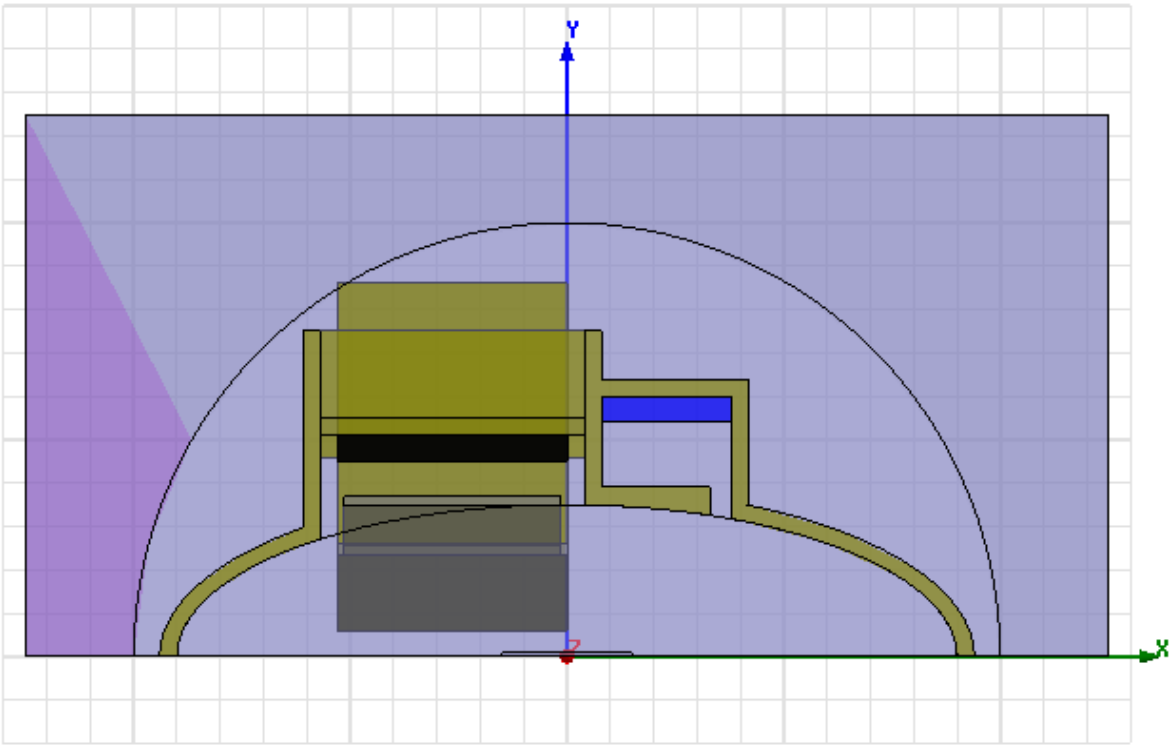

Figure 14 Cross-section of the improved design. Ferrites for damping the dipole and monopole trapped modes are shown in blue and black, respectively

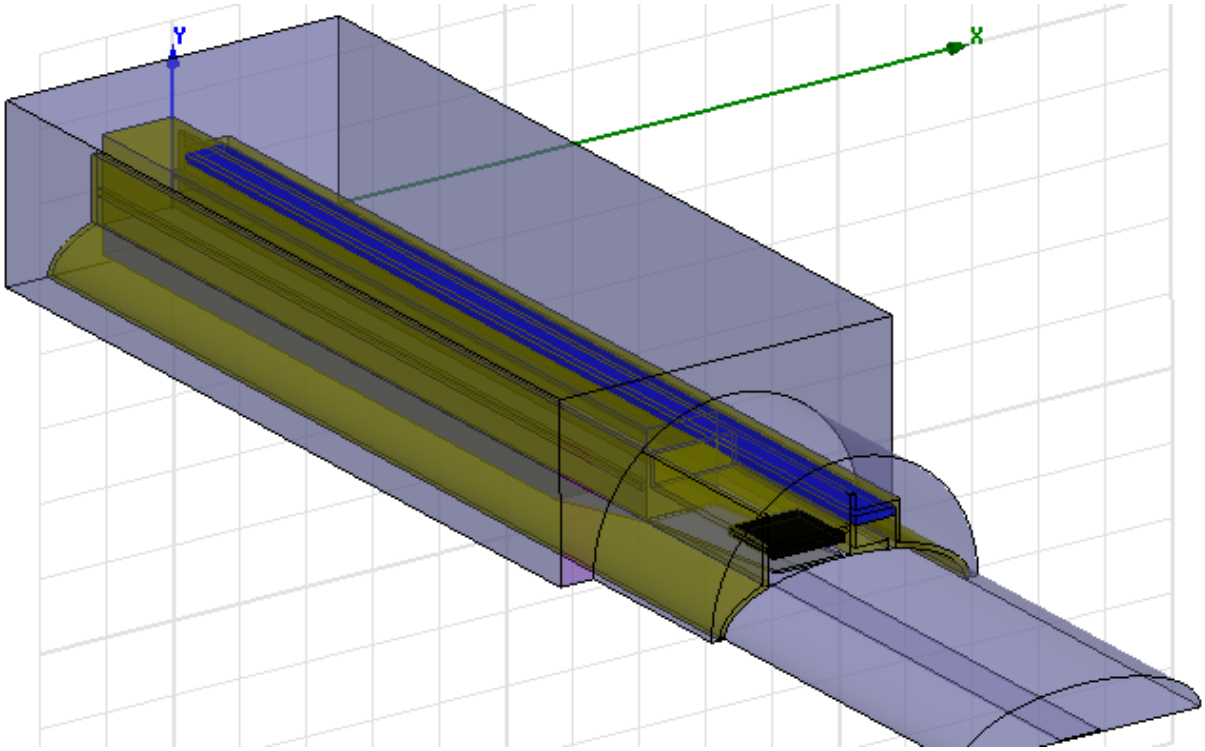

Figure 15 3D-view of the improved design. Ferrites for damping the dipole and monopole trapped modes are shown in blue and black, respectively.

3.1.3 Reduction of the impedance of the monopole trapped modes

In order to reduce the heat dissipated in the device and particularly in the rf-fingers, the shunt impedance of the monopole trapped modes must be reduced. Like for the dipole modes, this can be done by introducing ferrites where they do not perturb the beam image currents but damp the electromagnetic field of the monopole modes. As demonstrated in Fig. 6, the field of the most dangerous modes is mainly confined in the transition region in the vicinity of the longitudinal rf-fingers. Placing the ferrite in this region in such a way that it is shielded from the beams by the rf-fingers themselves solves the problem. The ferrite for damping the monopole modes is shown in black in Figs. 14 and 15.

3.1.4 Summary of the proposals concerning the device improvement

Several changes to the initial design are proposed in order to reduce the device impedance:

- Reduction of the tapering angle from 15 to 10 degree
- Limit minimum gap size to about 12 mm
- Create special damping chamber with ferrite along the whole device
- Place ferrite in the transition region next to the longitudinal rf-fingers

Modified geometry of the improved design is shown in Fig. 14 and 15.

3.2 Calculation of the impedances of the improved design

In this section, the results of the calculation of the longitudinal and transverse impedances of the improved design, shown in Figs. 14 and 15 are presented. These results should serve as a reference for estimating the impact of the TCTVBs and TCLIAs on the LHC beam stability.

3.2.1 The longitudinal broad-band geometrical impedance

The longitudinal broad-band geometrical impedance of the improved design is presented in Fig. 16. It is approximately two times smaller than the corresponding impedance of the initial design due to the improvements in the transition region. The values of the impedance for the minimum recommended gap of 12 mm are estimated as following:

- At injection: 2 TCLIAs have gap of 12 mm and 4 TCTVBs have gap of 60 mm. The beam goes through the half of the devices at the beam position 1 and through the other half at the beam position 2. This results in 0.135+0.55+2*(0.055+0.015) = 0.33 mΩ. It is less than 1 % of Total LHC budget of 70 mΩ at injection [8].

- At top energy: 2 TCLIAs have gap of 60 mm and 4 TCTVBs have gap of 12 mm. Again, the beam goes through the half of the devices at the beam position 1 and through the other half at the beam position 2. This results in 0.055+0.015+2*(0.135+0.055) = 0.45 mΩ. It is also less than 1 % of Total LHC budget of 76 mΩ at top energy [8].

Summarizing, the contribution of all 6 devices in the longitudinal geometrical broad-band impedance Z/n does not exceed 1 % of the total LHC budget both at injection and at top energy.

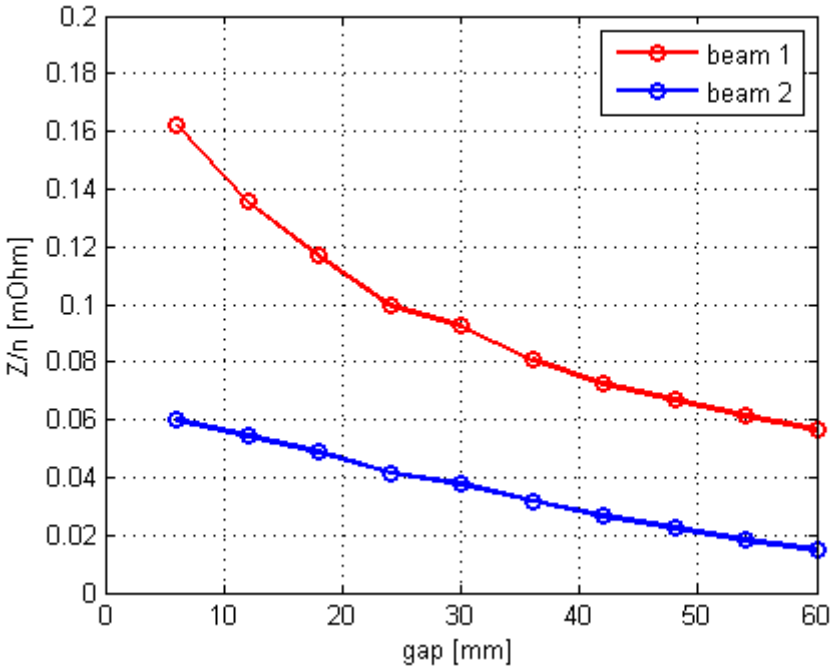

Figure 16 Longitudinal broad-band geometrical impedance of the improved design versus gap for both positions of the beam: 1 (red) and 2 (blue).

3.2.2 The transverse broad-band geometrical impedance

The transverse broad-band geometrical impedance of the improved design is presented in Fig. 17 for both positions of the beam: 1 (red) and 2 (blue). It is about 50 % higher than the corresponding impedance of the initial design due to the damping chamber, which increases the effective transverse cross-section of the devices. The impedance of all 6 devices is dominated by those with minimum gap and seen by the beam from position 1. Then the values of the impedance for the minimum recommended gap of 12 mm are estimated as follows:

- At injection: the beam goes through 1 TCLIAs which has gap of 12 mm at beam position 1. Taking into account the ratio of the local beta-function to the average one, this results in an effective impedance of 0.03•(130/70) = 0.055 MΩ/m. This is about 4 % of total LHC budget of 1.34 MΩ/m at injection [8].

- At top energy: the beam goes through 2 TCTVBs which have gap of 12 mm at beam position 1. Taking into account the ratio of the local beta-function to the average one, this results in an effective impedance of 2•0.03•(60/70) = 0.051 MΩ/m. This is about 2 % of total LHC budget of 2.67 MΩ/m at top energy [8].

Summarizing, the contribution of all 6 devices to the transverse geometrical broad-band impedance does exceed 1 % of the total LHC budget, both at injection and at top energy. To keep it under the 1 % limit, the gap should be increased up to 22 mm at injection and up to 16 mm at top energy.

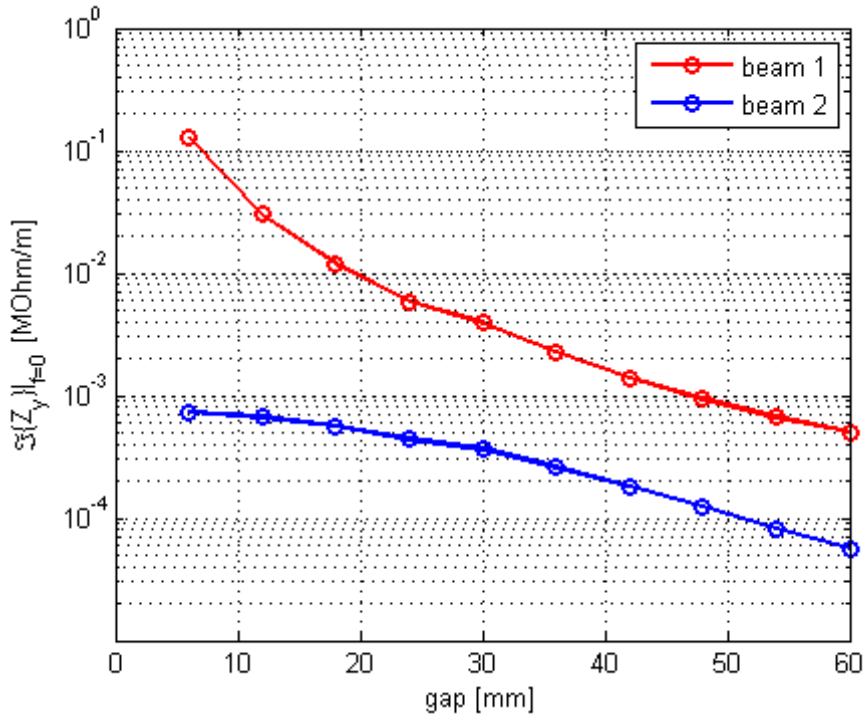

Figure 17 Transverse broad-band geometrical impedance of the improved design versus gap for both positions of the beam: 1 (red) and 2 (blue).

3.2.3 The impedance of the monopole trapped modes

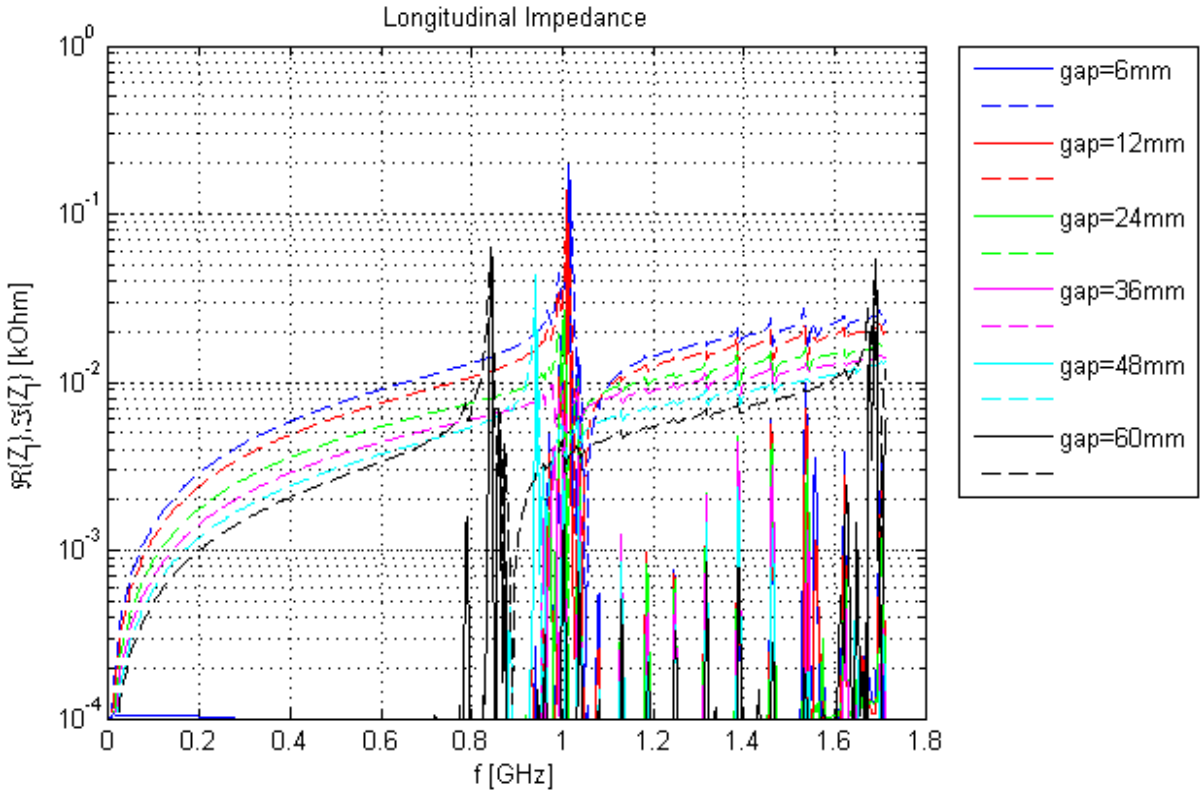

Figure 18 Longitudinal geometrical impedance of the improved design versus frequency for different values of the gap for beam position 1.

The longitudinal geometrical impedance of the improved design is presented in Fig. 18 for beam position 1 and for different gap sizes. The height of the peaks is proportional to the R/Q of the monopole trapped modes. In the improved design, the strongest mode is excited for 6 mm gap configuration at about 1 GHz. Increasing the gap up to 40 mm decreases the impedance of the trapped mode without changing its frequency. A further increase of the gap from 40 mm up to 60 mm increases the impedance and decreases the frequency at the same time. Finally, the strongest mode for the 60 mm gap configuration has an impedance which is only slightly smaller than for 6 mm gap configuration, but it has a lower frequency of about 0.85 GHz. That means that it is not clear from Fig. 18, in which case, 6 mm or 60 mm, power loss will be larger; both cases must be investigated.

In the case of 12 mm gap, the impedance of longitudinal trapped modes has been calculated using HFSS both with and without damping ferrites. The simulation of the improved design without ferrites shows very good agreement with the time domain simulation done using GdfidL (see results in Fig. 18). The strongest mode has been found at frequency f_0=1.009 GHz with quality factor Q_0=2800 (for TCTVB with W jaws), a shunt impedance R_0^{b1}=1.7 kΩ at the position of beam 1 and R_0^{b2}=0.5 kΩ at the position of beam 2, resulting in power losses of 80 Wand 24 W, respectively. As in the case of the longitudinal broad-band geometrical impedance, it is about factor 2 smaller than for the initial design. Still damping is necessary to reduce the power losses further. The simulation of the improved design with ferrites put in place (as it will be built) shows that the strongest mode is damped very efficiently. The frequency f_0=1.06 GHz is slightly modified and the quality factor Q_0=2.8 is reduced by 3 orders of magnitude. There is practically no power dissipation due to trapped modes.

The situation is very similar in the case of a 60 mm gap. Simulation of the improved design without ferrites shows again very good agreement with time domain simulations using GdfidL. The strongest mode is found at frequency f_0=0.842 GHz with a quality factor Q_0 =2200 (for TCTVB with W jaws), a shunt impedance R_0^{b1}=440 Ω at the position of beam 1 and R_0^{b2}=120 Ω at the position of beam 2, resulting in power losses of 51 W and 14 W, respectively. Again the damping works perfectly reducing quality factor of the mode again by a factor 1000. No significant power losses due to trapped modes have been found in the improved design with 60 mm gap.

References

[1] A. Bertarelli et al, 'The mechanical design for the LHC collimators', LHC-Project-Report-786, (2004).

[2] B. Goddard, 'Modification of TCLIA and TCTVB positions in IR2 and IR8', Engineering Change Order LHC-T-EC-0002, 2005-10-26, (EDMS No.: 671749).

[3] M. Mayer and R. Perret, Private communication, January 2006

[4] S. Radelli, Private communication, January 2006

[5] www.ansoft.com

[6] www.gdfidl.de

[7] S. Calatroni, R. Perret, W. Vollenberg, 'RF contacts for TCS collimators', TS-Note-2005-027, (EDMS No.: 550560).

[8] LHC Design Report, vol. 1, CERN-2004-003, Subsection 5.2.3, 2004.

[9] A. W. Chao, 'Physics of collective beam instabilities in high energy accelerators', John Wiley & Sons, New York, 1993.

[10] LHC Design Report, vol. 1, CERN-2004-003, Subsection 5.4.5, 2004.

[11] K. Yokoya, 'Impedance of slowly tapered structures', CERN-SL-90-88-AP, 1990.

[12] G. V. Stupakov, 'High-frequency impedance of small-angle collimators', In Proceedings of the 2001 PAC, Chicago, p. 1859, 2001.

[13] A. Grudiev, 'Simulation of longitudinal and transverse impedances of trapped modes in LHC secondary collimator', CERN-AB-Note-2005-042, 2005.